Journal of Alloys and Compounds 502 (2010) 97–106

Contents lists available at ScienceDirect

Journal of Alloys and Compounds

journal homepage: www.elsevier.com/locate/jallcom

Studies on optical absorption and photoluminescence properties of Pr^{3+} and Nd^{3+} doped mixed alkali chloroborate glasses

C. Venkateswarlu[a], G.N. Hemantha Kumar[a], M. Seshadri[a], Y.C. Ratnakaram[a,*], K.S.R. Koteswara Rao[b], J.L. Rao[a]

[a] Department of Physics, Sri Venkateswara University, Tirupati 517 502, India
[b] Department of Physics, Indian Institute of Science, Bangalore-560012, India

ARTICLE INFO

Article history:
Received 1 February 2010
Received in revised form 16 March 2010
Accepted 17 March 2010
Available online 23 March 2010

Keywords:
Borate glass
Absorption
Photoluminescence
Cross-section

ABSTRACT

This article presents the optical absorption and emission properties of Pr^{3+} and Nd^{3+} doped two different mixed alkali chloroborate glass matrices of the type $70B_2O_3{\cdot}xLiCl{\cdot}(30-x)NaCl$ and $70B_2O_3{\cdot}xLiCl{\cdot}(30-x)KCl$ (x = 5, 10, 15, 20 and 25). The variation of Judd–Ofelt parameters (Ω_2, Ω_4 and Ω_6), total radiative transition probabilities (A_T), radiative lifetimes (τ_R) and emission cross-sections (σ_p) with the variation of alkali contents in the glass matrix have been discussed in detail. The changes in the peak wavelengths of the hypersensitive transition and intensity parameters with x are correlated to the structural changes in the host matrix. The estimated radiative lifetimes of certain excited states of Pr^{3+} and Nd^{3+} in these two glass matrices are reported. Peak stimulated emission cross-sections (σ_P) are reported for the observed emission transitions of Pr^{3+} and Nd^{3+} ions. Branching ratios (β) of the observed emission transitions obtained from the Judd–Ofelt theory are compared with the values obtained from the emission spectra.

1. Introduction

Rare earth ions doped glassy matrices have become an attractive area of research due to their potential applications for optical telecommunications and laser technology [1,2]. Among different rare earth ions, Pr^{3+} has a unique feature which is due to close energy separation between the lower edge of the 4f5d configuration and ^1S_o level of $4f^2$ configuration. Pr^{3+} doped glasses find numerous applications such as UV–VIS–NIR lasers, up converters, optical fibers and optical amplifiers [3]. Pr^{3+} ion is considered as a promising activator for tunable UV solid state lasers, lamp phosphors, scintillation detectors, etc. [4,5]. Pr^{3+} ion has a very wide NIR spontaneous emission band (3.5–5.5μm), but it suffers from finding a suitable host material due to its tightly spaced energy levels (<2500 cm^{-1}) [6]. Among other rare earth ions, Nd^{3+} is the most widely investigated ion in a variety of glasses not only because of its applications but also because of the variations in its properties with composition. These properties include absorption and emission cross-sections, radiative and non-radiative transition rates and quantum efficiencies. Nd^{3+} ion has been recognized as one of the most efficient ions for obtaining laser emission in the NIR region [7–9].

A glass exhibits non-linear variation in its properties (that include density, viscosity, glass transition temperature and conductivity) when one alkali component in a multicomponent glass is systematically replaced by another species [10–12]. Besides the glasses containing only alkali ions, this non-linear behavior is exhibited by certain mixed alkali–alkaline earth oxide glasses also [13]. This phenomenon is referred to as 'mixed alkali effect' and is useful in manufacturing low loss electrical glass [10]. To study the mixed alkali phenomenon, borate glasses proved to be promising hosts to investigate the influence of chemical environment, structural diversity of ligand groups and spectroscopic properties of the materials [14]. For the alkali borate glasses, the abrupt changes in properties are observed near 15–20 mol% of modifier oxide [15,16]. In spite of numerous investigations, there appears to be no universally accepted mechanism for various mixed alkali effects.

It is well known that the radiative properties of rare earth ions in glass hosts can be described by the phenomenological application of Judd–Ofelt [17,18] theory. Earlier, the authors have studied the effect of mixed alkalis on absorption and photoluminescence spectra of Pr^{3+} and Er^{3+} doped borate glasses by employing Judd–Ofelt theory [19]. In the present work, the authors are interested to study the effect of mixed alkalis in two different chloroborate glass hosts using Pr^{3+} and Nd^{3+} as probing ions, keeping in view of the numerous applications of borate glasses. This work presents the results of investigations on the variation in Judd–Ofelt intensity parameters (Ω_2, Ω_4 and Ω_6), radiative lifetimes (τ_R) and emis-

* Corresponding author. Tel.: +91 877 2289472.
E-mail address: ratnakaram_yc@yahoo.co.in (Y.C. Ratnakaram).

0925-8388/$ – see front matter © 2010 Elsevier B.V. All rights reserved.
doi:10.1016/j.jallcom.2010.03.139

sion cross-sections (σ_p) with the variation of alkali contents in the glass matrix. The branching ratios (β) and integrated absorption cross-sections ($\sum$) have been computed for certain excited states of Pr^{3+} and Nd^{3+} in these mixed alkali chloroborate glass hosts. Emission spectra of these two rare earths doped two mixed alkali chloroborate glasses are also studied.

2. Experimental

Mixed alkali chloroborate glasses doped with Pr^{3+} and Nd^{3+} ions were prepared using standard melt quenching technique. The chemicals used in the present work are H_3BO_3, LiCl, NaCl, KCl, Pr_6O_{11} and Nd_2O_3 of 99.9% purity for preparing glass samples. The anhydrous chlorides were dried by heating the samples at appropriate temperatures under vacuum. A small amount of ammonium chloride was added to these dehydrated chlorides in order to remove impurities. About 6–10 g of batch compositions were mixed in a specially made clay crucible and heated for 2 h in an electric furnace initially at a temperature of 400 °C. Then the mixture was kept at 950 °C. The melt was thoroughly shaken at 15 min interval in order to ensure homogeneity. These melts were quenched between two preheated brass plates. The surfaces of the samples were polished to a uniform thickness of 1–2 mm. The glass compositions studied in the present work are

(1) $69.8B_2O_3{\cdot}xLiCl{\cdot}(30-x)NaCl.0.2Pr_6O_{11}$ and $69.8B_2O_3{\cdot}xLiCl{\cdot}(30-x)KCl.0.2Pr_6O_{11}$ (x = 5, 10, 15, 20 and 25);
(2) $69.8B_2O_3{\cdot}xLiCl{\cdot}(30-x)NaCl.0.2Nd_2O_3$ and $69.8B_2O_3{\cdot}xLiCl{\cdot}(30-x)KCl.0.2Nd_2O_3$ (x = 5, 10, 15, 20 and 25)

Refractive indices of the glass samples were measured by using Abbe refractometer using monobromonaphthalene as adhesive liquid while for density measurements; Archimedes principle was employed using xylene as immersion liquid. The rare earth ion concentrations were obtained using measured densities and molecular weights. The absorption spectra in the wavelength regions, 400–2200 nm (for Pr^{3+}) and 400–900 nm (for Nd^{3+}) have been recorded using JASCO V-570 spectrometer (spectral resolution 0.1 nm). The luminescence spectra were obtained using SPEX Fluorolog-2 fluorometer (Model-II), 444 nm being the excitation wavelength for Pr^{3+} and TRIX 550 monochromator with liquid nitrogen cooled under excitation wavelength 514 nm for Nd^{3+} (spectral resolution 1 nm).

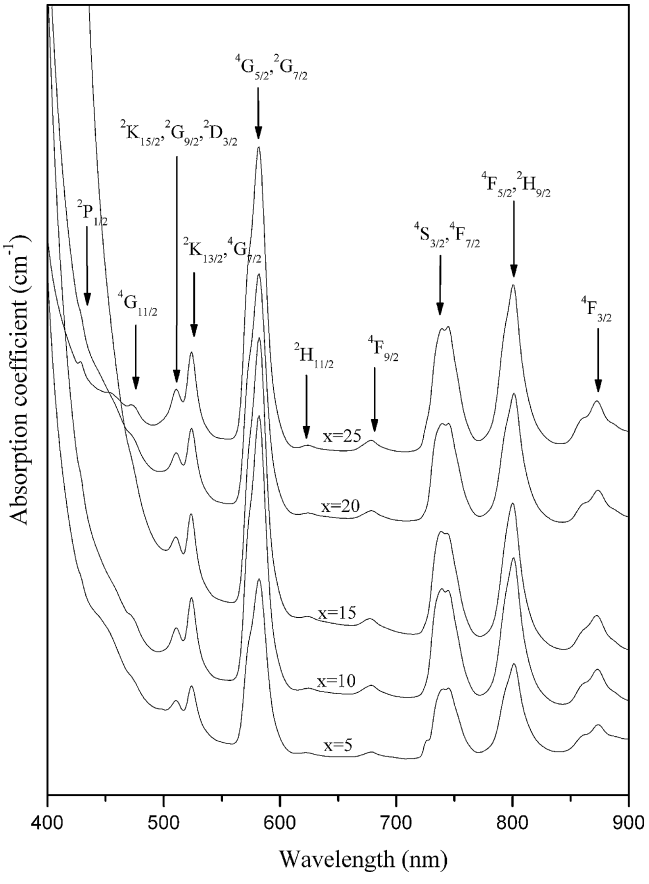

Fig. 1. Absorption spectra of Pr^{3+}doped lithium–sodium mixed alkali chloroborate glasses.

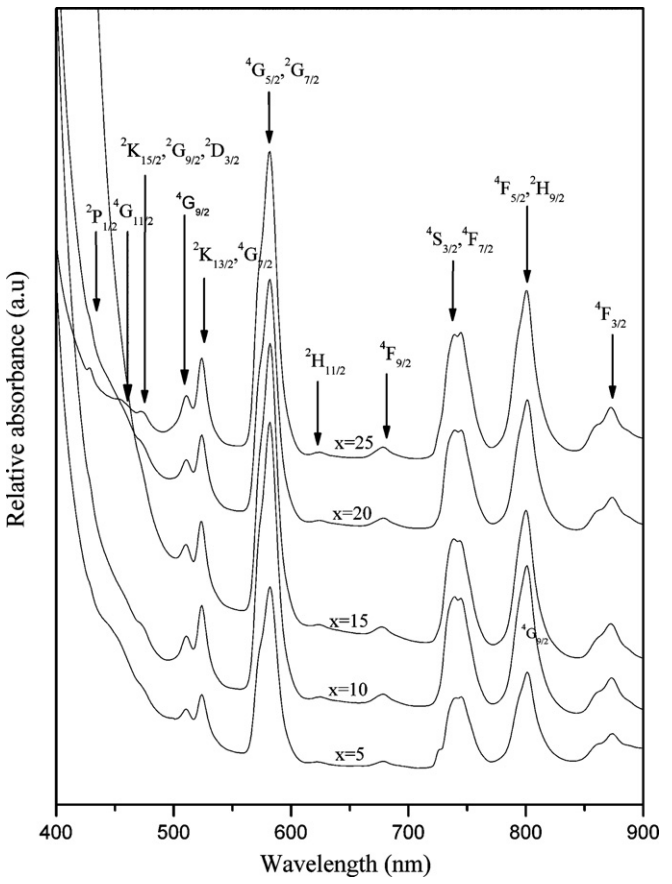

Fig. 2. Absorption spectra of Nd^{3+}doped lithium–sodium mixed alkali chloroborate glasses.

3. Results and discussion

3.1. Spectral intensities and intensity parameters

The room temperature optical absorption spectra of Pr^{3+} and Nd^{3+} ions doped lithium–sodium chloroborate (LSCB) glass are shown in Figs. 1 and 2 respectively. Similar spectra have been obtained in lithium–potassium glass (LPCB) for both the ions. Hence the spectra have not shown. In the case of Pr^{3+} ion, seven absorption peaks are observed for all the glass compositions of both LSCB and LPCB glasses. These absorption peaks correspond to transitions from the ground state, $^3H_4$ to various excited states. The observed band energies are compared with the calculated band energies (using the method described in Ref. [20]) and a good agreement is found between them. In the case of Nd^{3+} ion, eight absorption peaks are observed for all the glass compositions of both LSCB and LPCB glasses. In addition to these peaks, some more absorption peaks (as shown in Fig. 2) are observed for certain glass compositions. These absorption peaks correspond to transitions from the ground state, $^4I_{9/2}$ to various excited states. From the observed band energies, Racah (E^1, E^2 and E^3), spin–orbit interaction (ξ_{4f}), configuration interaction (α) (for Nd^{3+} ion only) parameters and hydrogenic ratios (E^1/E^3 and E^2/E^3) are evaluated for both Pr^{3+} and Nd^{3+} ions in these glass matrices and are presented in Table 1. From the table, it is observed that the changes in E^2 and E^3 parameters for both Pr^{3+} and Nd^{3+} ions are very small for different x values in both LSCB and LPCB glass matrices. The

Table 1
Racah (E^1, E^2, E^3), spin–orbit interaction (ξ_{4f}) and configuration interaction (α) parameters and hydrogenic ratios of Pr^{3+} and Nd^{3+} doped mixed alkali chloroborate glasses.

S. no.	Parameter	Lithium–sodium					Lithium–potassium				
		$x=5$	$x=10$	$x=15$	$x=20$	$x=25$	$x=5$	$x=10$	$x=15$	$x=20$	$x=25$
Praseodymium											
1	E^1	4603.0	4472.6	4564.9	4527.4	4531.1	4450.6	4517.8	4573.8	4571.0	4582.7
2	E^2	21.7	21.9	21.8	22.3	22.3	22.6	22.0	21.7	21.8	21.9
3	E^3	456.3	454.0	454.3	455.7	456.3	455.6	454.6	454.9	455.9	456.0
4	ξ_{4f}	830.5	860.7	839.9	834.9	827.9	834.0	848.2	836.8	837.4	833.6
5	E^1/E^3	10.08	9.85	10.04	9.93	9.92	9.76	9.93	10.05	9.74	10.04
6	E^2/E^3	0.04	0.04	0.04	0.04	0.04	0.04	0.04	0.04	0.04	0.004
Neodymium											
1	E^1	5119.2	5086.5	5099.6	5111.4	5036.0	5075.1	5134.2	5070.4	5054.3	5045.6
2	E^2	23.1	23.1	22.7	23.1	23.9	23.3	22.6	23.4	23.6	23.9
3	E^3	489.5	488.8	488.4	489.5	491.5	489.4	487.2	491.2	490.9	492.6
4	ξ_{4f}	859.5	865.5	862.5	860.1	891.5	866.5	855.2	868.5	872.3	885.4
5	α	−1.97	−2.74	−3.57	−2.23	−0.52	−2.44	−4.55	−0.72	−0.48	−0.72
6	E^1/E^3	10.46	10.40	10.44	10.44	10.24	10.37	10.53	10.32	10.29	10.24
7	E^2/E^3	0.05	0.05	0.04	0.04	0.05	0.04	0.04	0.04	0.05	0.05

hydrogenic ratios (E^1/E^3 and E^2/E^3) for both the ions are nearly same for all the glass compositions indicating unperturbed radial properties.

The experimental (f_{exp}) and calculated (f_{cal}) spectral intensities of the observed absorption bands of Pr^{3+} and Nd^{3+} ions doped LSCB and LPCB glasses are obtained using the procedure explained in Ref. [20]. For calculating the spectral intensities of the overlapped peaks, the areas of the peaks are estimated by extrapolating up to the baseline. The experimental spectral intensities of the observed bands of Pr^{3+} and Nd^{3+} ions in these two glass matrices are presented in Table 2 for all the compositions studied. It is observed that for both Pr^{3+} and Nd^{3+} ions in these two glass matrices, there is a good agreement between the experimental and calculated spectral intensities and the RMS deviations are small confirming the validity of approximations made in the Judd–Ofelt theory. For Pr^{3+} ion, the spectral intensities are found to be higher at $x=25$ mol% (lithium rich) and lower at $x=5$ mol% (sodium rich) for all the excited states in LSCB glass. In case of LPCB glass, the spectral intensities are found to be higher at $x=5$ mol% (potassium rich). These results indicate higher crystal field asymmetries at $x=25$ mol% in LSCB glass and at $x=5$ mol% in LPCB glass. The best set of Judd–Ofelt intensity parameters (Ω_2, Ω_4 and Ω_6) of Pr^{3+} and Nd^{3+} doped LSCB and LPCB glasses are obtained using the formulae given in Ref. [20] and are presented in Table 3. These intensity parameters depend on the host glass composition [21]. Out of the three intensity parameters, Ω_2 parameter is related to covalency and structural changes in the vicinity of the rare earth ions whereas Ω_4 and Ω_6 parameters are indicative of rigidity of the medium. In the present work, it is observed that the covalency between Pr^{3+} cation and oxygen anion is lower (high ionicity) at $x=15$ mol% (as Ω_2 parameter is small) in both LSCB and LPCB glasses. It was suggested by Oomen and Van Dongen [22] that sometimes it is useful to observe the variation of the sum of the Judd–Ofelt intensity parameters, $\sum\Omega_\lambda$ with the variation in covalency. In the present work, $\sum\Omega_\lambda$ parameter (shown in Table 3) follows the same trend as the Ω_2 parameter in LSCB glass. In the case of LPCB glass, $\sum\Omega_\lambda$ gradually decreases with an increase in lithium content from $x=5$ mol% to 20 mol% and shows an increment at $x=25$ mol%. Variation of Ω_2 and $\sum\Omega_\lambda$ parameters with x in the glass matrix is shown in Fig. 3 for both the glasses.

In the case of Nd^{3+} ions, for most of the transitions, the spectral intensities are found to be lower at $x=5$ mol% (sodium rich) in LSCB glass and at $x=10$ mol% in LPCB glass indicating lower crystal field asymmetries at these compositions. The spectral intensities are higher at $x=15$ mol% in LPCB glass indicating higher crystal field asymmetry. From the magnitude of Judd–Ofelt intensity parameters, for Nd^{3+} ion, it is observed that the covalency is lower (as Ω_2 parameter is small) at $x=20$ mol% in LSCB glass and at $x=10$ mol% in LPCB glass. The sum of the intensity parameters, $\sum\Omega_\lambda$ follows the same trend as the Ω_2 parameter in both LSCB and LPCB glass matrices. The rigidity of the glass matrix is lower (as Ω_6 parameter is small) at $x=5$ mol% in LSCB glass and at $x=10$ mol% in LPCB glass. Variation of Ω_2 and $\sum\Omega_\lambda$ parameters with x in the glass matrix in both the glass matrices is shown in Fig. 4.

3.2. Hypersensitive transitions

The spectral intensities of certain transitions of rare earth ions are sensitive to the environment. These transitions are called as hypersensitive transitions [21]. $^3H_4 \rightarrow {}^3F_2$ is the hypersensitive transition for the Pr^{3+} ion and $^4I_{9/2} \rightarrow {}^4G_{5/2} + {}^2G_{7/2}$ is the hypersensitive transition for Nd^{3+} ion. Normally, the position and intensities of the hypersensitive transitions are largely dependent on the local environment of the rare earth ion and in turn affects the magnitude of intensity parameters. The shift in the peak wavelength of the hypersensitive transition towards shorter wavelength with the increase of x because of nephelauxetic effect [21] indicates that the degree of covelancy of R–O bond decreases with increasing x. Peak wavelengths of the hypersensitive transition (λ_P) and Ω_2 parameters of Pr^{3+} ions in LSCB and LPCB glasses in different compositions are given below.

x (in mol%)	Wavelength (nm)		Ω_2 ($\times10^{20}$ cm^2)	
	LSCB	LPCB	LSCB	LPCB
5	1916.0	1901.5	14.01	31.81
10	1916.1	1908.3	29.81	24.96
15	1908.5	1908.0	9.62	12.61
20	1900.5	1912.9	17.95	21.56
25	1909.4	1900.5	37.31	23.57

From the above data it is observed that in LSCB glass, there is a shift in hypersensitive band towards shorter wavelength (1908.5–1900.5 nm) with an increase of x from 15 mol% to 20 mol% but the Ω_2 parameter increased largely. This indicates some structural changes in LSCB glass matrix between $x=15$ mol% and $x=20$ mol%. In case of LPCB glass, structural changes are observed at $x=5$–10 mol% from the variation of peak wavelength of the hypersensitive transition and Ω_2 parameter. In the case of Nd^{3+} ions, in both the glass matrices, variation in covalency (Ω_2 parameter) is similar to the variation in the intensities of the hypersensitive transition for different x values in the glass matrix. Peak wavelengths of

Table 2
Experimental spectral intensities (f_{exp}) of certain excited states of Pr^{3+} ($f_{exp} \times 10^5$) and Nd^{3+} ($f_{exp} \times 10^6$) doped mixed alkali chloroborate glasses.

S. no.	Excited level	Lithium–sodium					Lithium–potassium				
		$x=5$	$x=10$	$x=15$	$x=20$	$x=25$	$x=5$	$x=10$	$x=15$	$x=20$	$x=25$
Praseodymium											
1	$^3F_2$	1.01	1.86	1.42	2.19	3.28	3.03	2.19	1.58	1.84	1.81
2	$^3F_3 + {}^3F_4$	3.11	5.82	4.62	6.79	11.33	8.32	6.39	5.69	4.29	5.56
3	$^1G_4$	0.05	0.41	0.05	0.12	0.19	0.14	0.10	0.09	0.08	0.86
4	$^1D_2$	0.58	0.90	0.84	1.15	1.68	1.11	1.06	0.99	0.83	0.77
5	$^3P_0$	0.33	0.64	1.23	1.48	1.61	1.69	1.08	1.05	0.78	0.66
6	$^3P_1 + {}^1I_6$	0.41	0.58	1.74	2.47	2.01	2.68	1.62	1.66	1.62	0.87
7	$^3P_2$	1.27	1.34	3.39	4.76	5.47	5.26	2.40	3.54	3.19	2.53
	Rms deviation	±0.15	±0.50	±0.85	±1.13	±0.69	±1.16	±0.19	±0.71	±2.36	±0.27
Neodymium											
1	$^4F_{3/2}$	2.23	3.45	3.69	3.23	3.78	2.87	3.18	3.33	3.00	3.13
2	$^4F_{5/2}, {}^2H_{9/2}$	10.07	15.90	16.21	14.80	14.20	14.20	8.22	15.31	12.60	12.70
3	$^4F_{7/2}, {}^4S_{3/2}$	11.30	18.70	16.64	14.81	15.03	15.11	9.38	17.70	13.41	11.90
4	$^4F_{9/2}$	0.89	1.65	2.20	1.24	1.44	1.39	0.82	1.44	1.14	1.31
5	$^2H_{11/2}$	0.29	0.51	0.51	0.34	0.44	0.43	0.20	0.59	0.33	0.33
6	$^4G_{5/2}, {}^2G_{7/2}$	33.70	57.30	53.62	36.30	68.60	44.82	24.61	48.70	45.40	39.60
7	$^2K_{13/2}, {}^4G_{7/2}$	6.19	10.40	7.93	8.56	12.01	8.10	3.36	8.86	7.81	7.10
8	$^4G_{9/2}$	3.11	4.49	3.26	4.18	5.32	4.24	0.92	4.52	4.61	4.68
9	$^2K_{15/2}, {}^2G_{9/2}, {}^2D_{3/2}$	–	0.73	–	0.67	1.19	0.67	–	0.72	0.52	1.02
10	$^4G_{11/2}$	–	–	–	–	0.82	–	–	–	–	0.81
11	$^2P_{1/2}$	–	–	–	–	0.73	0.82	–	–	0.56	0.47
	Rms deviation	±0.57	±0.87	±0.98	±0.91	±0.98	±0.82	±0.94	±0.87	±0.95	±0.95

Table 3
Judd–Ofelt intensity parameters ($\Omega_\lambda \times 10^{20}$) ($cm^2$) of Pr^{3+} and Nd^{3+} doped mixed alkali chloroborate glasses.

S. no.	Parameter	Lithium–sodium					Lithium–potassium				
		$x=5$	$x=10$	$x=15$	$x=20$	$x=25$	$x=5$	$x=10$	$x=15$	$x=20$	$x=25$
Praseodymium											
1	Ω_2	14.01	29.80	9.62	17.95	37.31	31.81	24.96	12.61	21.56	23.57
2	Ω_4	3.18	0.608	17.75	23.24	18.22	25.02	14.92	15.53	13.86	7.21
3	Ω_6	19.93	38.75	26.61	39.43	71.53	48.59	38.48	34.74	24.49	35.20
4	$\Sigma\Omega_\lambda$	27.12	69.16	53.98	80.62	127.06	105.42	78.36	62.87	59.91	65.98
Neodymium											
1	Ω_2	9.41	17.09	15.34	8.79	20.16	12.59	6.32	14.05	12.84	10.07
2	Ω_4	4.30	5.52	6.28	6.84	7.73	5.58	4.03	5.37	5.64	6.75
3	Ω_6	7.77	12.51	11.49	10.2	9.80	10.32	6.05	11.85	9.01	8.21
4	$\Sigma\Omega_\lambda$	21.48	35.12	33.11	25.83	37.69	28.49	16.40	31.27	27.49	25.03

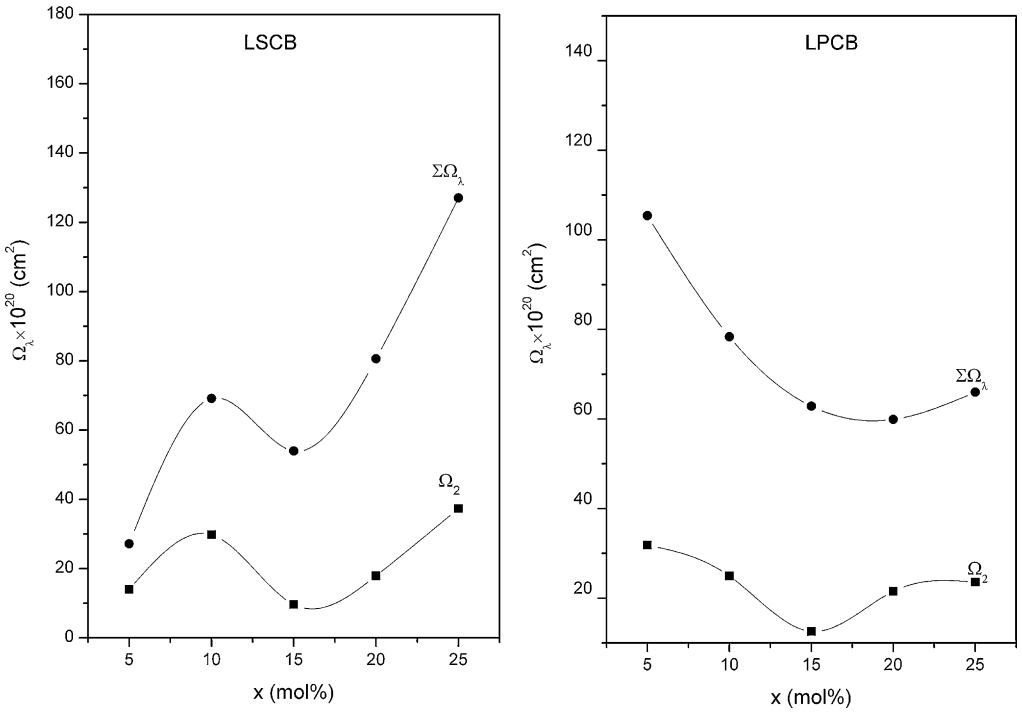

Fig. 3. Variation of Ω_2 and $\Sigma\Omega_\lambda$ parameters with x in Pr^{3+} doped lithium–sodium (LSCB) and lithium–potassium (LPCB) mixed alkali chloroborate glasses.

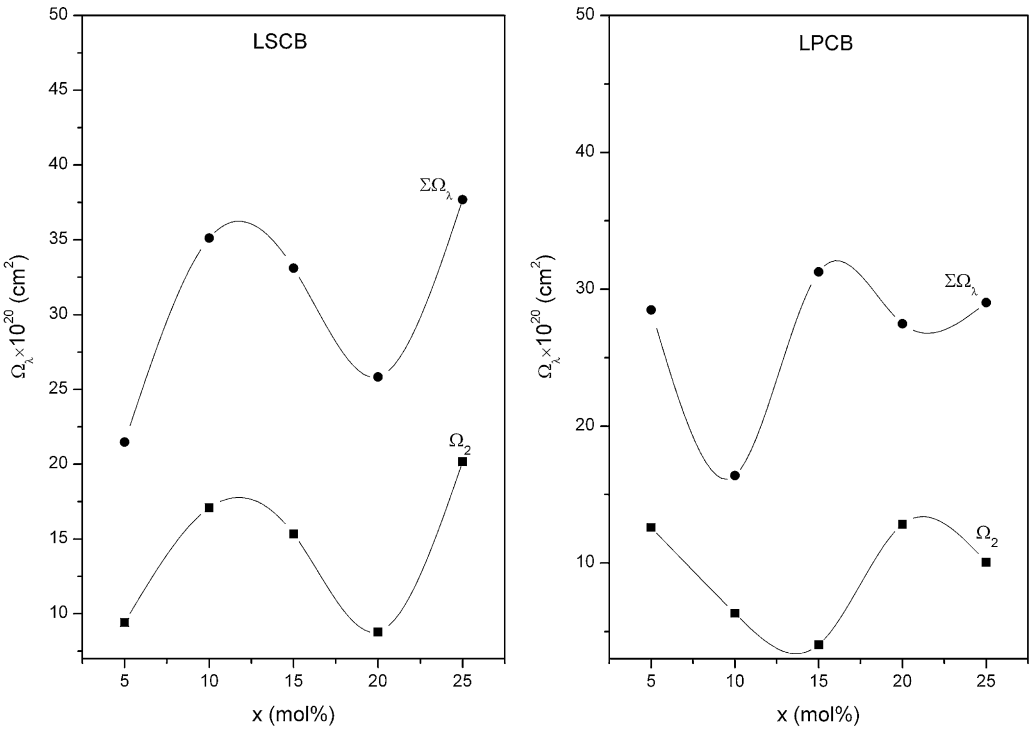

Fig. 4. Variation of Ω_2 and $\Sigma\Omega_\lambda$ parameters with x in Nd^{3+} doped lithium–sodium (LSCB) and lithium–potassium (LPCB) mixed alkali chloroborate glasses.

the hypersensitive transition (λ_P) and Ω_2 parameters of Nd^{3+} ions in LSCB and LPCB glasses in different compositions are given below.

x (in mol%)	Wavelength (nm)		Ω_2 ($\times 10^{20}$ cm^2)	
	LSCB	LPCB	LSCB	LPCB
5	582.1	582.2	9.41	12.59
10	581.8	583.6	17.09	6.32
15	582.0	581.8	15.34	14.05
20	582.1	581.6	8.79	12.84
25	581.4	580.4	20.16	10.07

From the above data, it is observed that in the case of Nd^{3+} doped LSCB glass, the change in peak wavelength of the hypersensitive transition with x in the glass matrix is very small indicating that structural changes are not influencing the covalency of Nd–O bond. In case of LPCB glass, some structural changes were observed at x = 10–15 mol%. The spectral profiles of the hypersensitive transitions appeared to be same for both Pr^{3+} and Nd^{3+} ions in LSCB and LPCB glass hosts at different compositions.

3.3. Radiative lifetimes

Radiative lifetimes (τ_R), branching ratios (β) and integrated absorption cross-sections ($\sum$) for certain excited states of Pr^{3+} and Nd^{3+} doped LSCB and LPCB glass matrices are evaluated using the formulae given in Ref. [23]. Estimated radiative lifetimes (τ_R) of the excited states, $^3P_1$, $^3P_0$, $^1D_2$ and $^3F_3$ of Pr^{3+} ion in LSCB and LPCB glasses are presented in Table 4. It is observed that the magnitudes of radiative lifetimes for these excited states are higher at x = 5 mol% (sodium rich) and lower at x = 25 mol% (lithium rich) in LSCB glass. In the case of LPCB glass, the radiative lifetimes of all the excited states are lower at x = 5 mol% (potassium rich). Among these four excited states, $^3F_3$ shows significantly higher radiative lifetimes in both the glass matrices at all the glass compositions. The branching ratios (β) and integrated absorption cross-sections ($\sum$) for certain transitions of Pr^{3+} ions which are observed in emission spectra are presented in Table 5. It is observed that among the five glass compositions studied, $^3P_0 \rightarrow {}^3H_4$ transition has higher branching ratio at x = 15 mol% in LSCB glass. These studies suggest

Table 4
Radiative lifetimes (τ_R) (μs) of certain excited states of Pr^{3+} and Nd^{3+} doped mixed alkali chloroborate glasses.

S. no.	Excited level	Lithium–sodium					Lithium–potassium				
		x = 5	x = 10	x = 15	x = 20	x = 25	x = 5	x = 10	x = 15	x = 20	x = 25
Praseodymium											
1	$^3P_1$	12.1	7.2	6.7	4.5	3.4	3.6	5.1	6.3	6.0	6.6
2	$^3P_0$	11.9	7.4	6.5	4.4	3.4	3.5	4.9	6.3	5.8	6.5
3	$^1D_2$	90.4	48.4	73.9	46.3	27.9	33.5	44.8	63.2	55.9	50.9
4	$^3F_3$	419.9	233.5	278.9	187.1	119.1	149.2	200.2	235.7	275.3	235.2
Neodymium											
1	$^4G_{9/2}$	47.9	29.2	30.5	41.8	24.8	36.4	63.6	33.5	36.3	40.3
2	$^4G_{7/2}$	50.3	30.0	32.0	45.4	25.5	37.8	68.2	34.7	37.8	42.7
3	$^4G_{5/2}$	32.9	19.5	20.8	29.9	16.4	24.7	45.0	22.6	24.5	27.7
4	$^2H_{11/2}$	1626.3	1011.4	1077.2	1406.0	885.1	1270.2	2230.6	1160.6	1290.0	1425.9
5	$^4F_{9/2}$	203.2	131.0	136.5	151.0	149.4	153.8	253.7	137.7	172.8	179.1
6	$^4F_{5/2}$	173.5	114.1	117.4	126.0	122.1	131.0	211.3	119.1	145.0	144.7
7	$^4F_{3/2}$	229.7	152.7	155.0	164.3	157.9	173.5	275.0	159.4	190.1	187.0

Table 5
Branching ratios (β) and integrated absorption cross-sections (Σ) of the observed emission transitions of Pr^{3+} and Nd^{3+} in lithium–sodium and lithium–potassium chloroborate glasses.

S. no	Transition	Parameter	Lithium–sodium					Lithium–potassium				
			$x=5$	$x=10$	$x=15$	$x=20$	$x=25$	$x=5$	$x=10$	$x=15$	$x=20$	$x=25$
Praseodymium												
1	$^3P_0 \rightarrow {}^3H_4$	β	0.176	0.20	0.521	0.497	0.286	0.395	0.339	0.442	0.370	0.219
		Σ	16.50	3.12	91.03	120.22	94.35	129.13	76.99	79.76	71.64	37.41
2	$^1D_2 \rightarrow {}^3H_4$	β	0.304	0.297	0.370	0.344	0.345	0.300	0.308	0.388	0.260	0.309
		Σ	34.06	65.53	45.02	67.28	122.19	82.70	65.46	58.80	41.75	60.19
Neodymium												
1	$^4F_{3/2} \rightarrow {}^4I_{9/2}$	β	0.353	0.327	0.352	0.379	0.400	0.352	0.379	0.330	0.371	0.409
		Σ	5.78	8.02	8.49	8.69	9.48	7.58	5.15	7.74	7.32	8.18
2	$^4F_{3/2} \rightarrow {}^4I_{11/2}$	β	0.533	0.553	0.534	0.516	0.500	0.535	0.515	0.550	0.521	0.495
		Σ	12.8	19.93	18.92	17.37	17.31	16.95	10.30	18.98	15.14	14.58
3	$^4F_{3/2} \rightarrow {}^4I_{13/2}$	β	0.109	0.115	0.109	0.101	0.095	0.108	0.101	0.114	0.103	0.093
		Σ	4.29	6.88	6.34	5.62	5.43	5.68	3.33	6.53	4.95	4.51

that the transition, $^3P_0 \rightarrow {}^3H_4$ at $x=15$ mol% may be suitable for laser excitation.

Radiative lifetimes of the excited states, $^4G_{9/2}$, $^4G_{7/2}$, $^4G_{5/2}$, $^2H_{11/2}$, $^4F_{9/2}$, $^4F_{5/2}$ and $^4F_{3/2}$ of Nd^{3+} ions in LSCB and LPCB glass matrices are estimated and are given in Table 4. It is observed that the radiative lifetimes of all the excited states are higher at $x=5$ mol% (sodium rich) and lower for some of the excited states at $x=25$ mol% in LSCB glass. In the case of LPCB glass, the radiative lifetimes are found to be higher at $x=10$ mol% and lower at $x=15$ mol%. The branching ratios (β) and integrated absorption cross-sections ($\sum$) for certain transitions, which are observed in emission spectra are presented in Table 5. It is observed that the transition, $^4F_{3/2} \rightarrow {}^4I_{11/2}$ has higher branching ratios when compared with other transitions in both the glass matrices. Among different compositions studied, this transition has higher branching ratio at $x=10$ mol% in LSCB glass. The integrated absorption cross-sections ($\sum$) are also higher for this transition at $x=10$ mol%. In the case of LPCB glass, the transition, $^4F_{3/2} \rightarrow {}^4I_{11/2}$ shows higher branching ratio at $x=15$ mol%. Therefore, at $x=10$ mol% in LSCB glass and at $x=15$ mol% in LPCB glass, the transition, $^4F_{3/2} \rightarrow {}^4I_{11/2}$ may be favorable for laser excitation. Variation of total radiative transition probabilities (A_T) of certain excited states of Pr^{3+} and Nd^{3+} with x in the glass matrix is shown in Fig. 5.

3.4. Non-radiative properties

The exponential dependence of the multiphonon relaxation rate, W_{MPR} on the energy gap to the next lower level ΔE has been experimentally established for a number of crystals and glasses and is given by Ref. [24]

$$W_{MPR} = C \exp[-\alpha \Delta E](n(\omega, p) + 1)^p \quad (1)$$

where C and α are positive, host dependent constants, which are almost independent of the specific 4f level of trivalent rare earth ions except in a few cases, ΔE is the energy gap between the emitting and closest lower electronic level, ω the stretching frequency of the glass forming groups and $P = \Delta E/\hbar\omega$ the number of phonons which must be emitted in order to conserve energy during the transition. The explicit temperature dependence of W_{MPR} through the Bose–Einestein occupation number, $n = 1/(\exp(\hbar\omega/KT) - 1)$ provides a way to determine the number and energy of the phonons involved in the decay process. In the present work, non-radiative relaxation rate constants (W_{MPR}) were calculated for various Pr^{3+} excited states in these mixed alkali chloroborate glasses (using the values $\alpha = 3.8 \times 10^{-3}$ cm^{-1} and $C = 2.9 \times 10^{-12}$ s^{-1} reported for borate glasses [25]) and are presented in Table 6 for all the glasses studied.

3.5. Luminescence spectra

Fig. 6 shows the photoluminescence spectra of Pr^{3+} (under the excitation wavelength, 444 nm) and Nd^{3+} (under the excitation wavelength, 514 nm) doped LSCB glass matrix for different x values in the glass matrix. Similar spectra have been observed in the case of LPCB glass. Hence the spectra are not shown. The spectra exhibit two emission peaks corresponding to the transitions, $^3P_o \rightarrow {}^3H_4$ and $^1D_2 \rightarrow {}^3H_4$ nearly at 490 nm and 603 nm respectively in all the compositions. It is observed that the intensity of the peak corresponding to the transition, $^3P_o \rightarrow {}^3H_4$ is found to be more in LPCB glass as compared to LSCB glass except at $x=15$ mol% and 20 mol%. It is also observed that the intensity of the transition, $^1D_2 \rightarrow {}^3H_4$ is found to be increased with the increase of x from 5 mol% to 25 mol% in LPCB glass. The peak stimulated emission cross-sections (σ_p) for the two emissions have been evaluated using the formula given in Ref. [26]. Table 7 presents peak stimulated emission cross-sections (σ_p) for the above two transitions of Pr^{3+} in LSCB and LPCB glass matrices. It is observed that the emission cross-section for the transition, $^3P_o \rightarrow {}^3H_4$ is more at $x=20$ mol% in LSCB glass and at $x=5$ mol% (potassium rich) in LPCB glass. For $^1D_2 \rightarrow {}^3H_4$ transition, σ_p value is higher at $x=25$ mol% (lithium rich) and at $x=5$ mol% (potassium rich) in these two glass matrices. The emission cross-section for the transition, $^3P_o \rightarrow {}^3H_4$ obtained in the present work is slightly of higher order when compared to those reported by Srinivasa Rao et al. [27] in alkali borate glasses.

In the case of Nd^{3+} ions, the spectra exhibit three emission peaks corresponding to transitions, $^4F_{3/2} \rightarrow {}^4I_{9/2}$, $^4F_{3/2} \rightarrow {}^4I_{11/2}$ and $^4F_{3/2} \rightarrow {}^4I_{13/2}$ nearly at 905 nm, 1080 nm and 1350 nm respectively. The peak stimulated emission cross-sections (σ_p) are calculated for these three emission peaks and are presented in Table 7 for all the compositions. Among these three emission transitions, the transition, $^4F_{3/2} \rightarrow {}^4I_{11/2}$ has higher magnitudes of cross-section when compared to the other two transitions in both the glasses. This transition has higher emission cross-section at $x=10$ mol% in LSCB glass and at $x=15$ mol% in LPCB glass. Hence, the transition, $^4F_{3/2} \rightarrow {}^4I_{11/2}$ at $x=15$ mol% in LPCB glass is more suitable for laser excitation in view of its better emission cross-section. From the emission spectra of Pr^{3+} and Nd^{3+} ions, branching ratios of the observed emission transitions are obtained from the areas of the emission peaks exper-

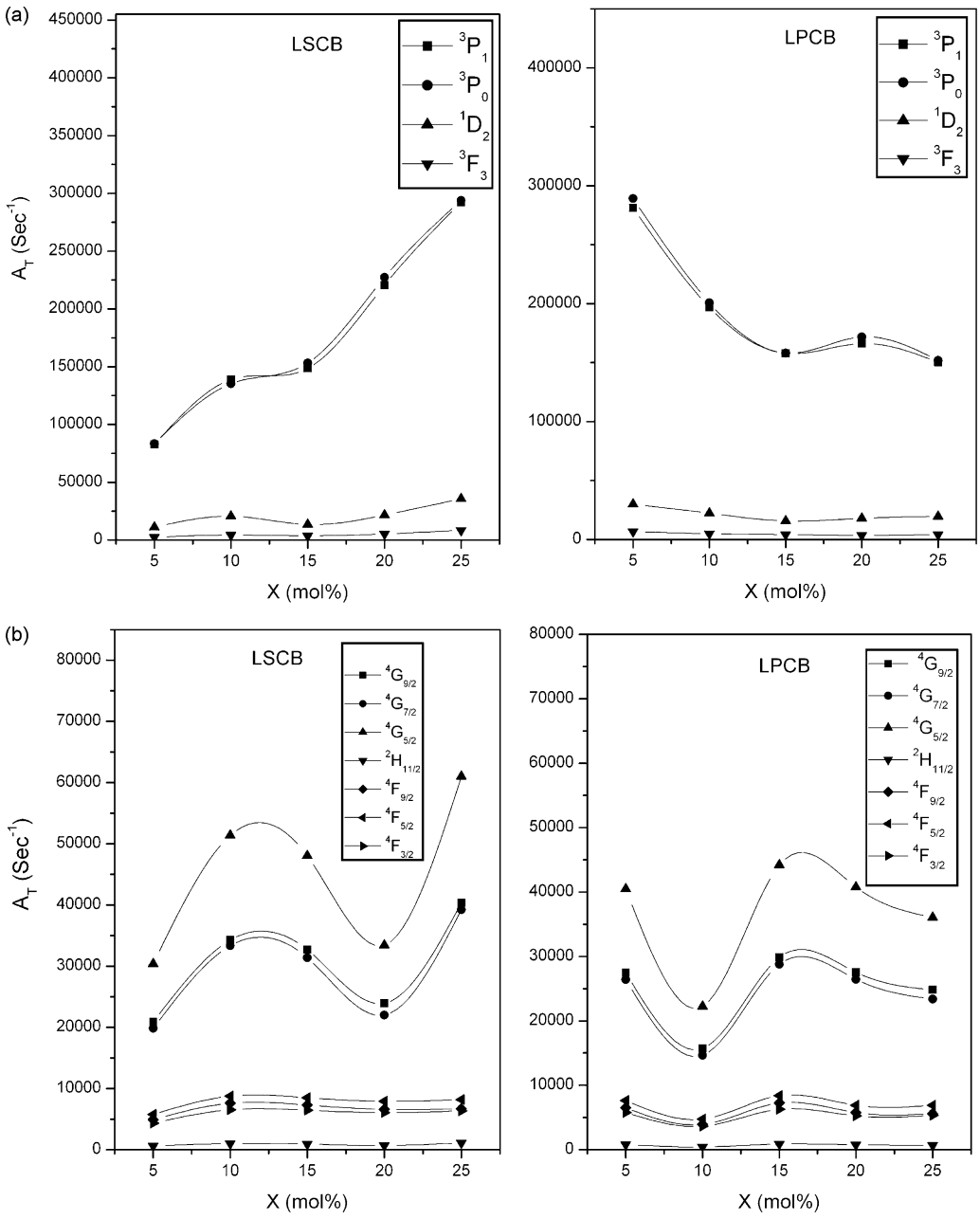

Fig. 5. (a) Variation of A_T with x in Pr^{3+} doped lithium–sodium (LSCB) and lithium–potassium (LPCB) mixed alkali chloroborate glasses. (b) Variation of A_T with x in Nd^{3+} doped lithium–sodium (LSCB) and lithium–potassium (LPCB) mixed alkali chloroborate glasses.

Table 6
Non-radiative relaxation rates (W_{MPR}) (s^{-1}) of certain transitions of Pr^{3+} doped mixed alkali chloroborate glasses.

Transition	Lithium-sodium					Lithium–potassium				
	$x=5$	$x=10$	$x=15$	$x=20$	$x=25$	$x=5$	$x=10$	$x=15$	$x=20$	$x=25$
$^3P_2 \rightarrow {}^1I_6$	6.18×10^{10}	3.25×10^{10}	6.67×10^{10}	5.88×10^{10}	5.86×10^{10}	6.49×10^{10}	5.23×10^{10}	6.93×10^{10}	6.33×10^{10}	5.86×10^{10}
$^1I_6 \rightarrow {}^3P_1$	1.43×10^{12}	1.44×10^{12}	1.02×10^{12}	1.26×10^{12}	1.29×10^{12}	1.37×10^{12}	1.27×10^{12}	1.27×10^{12}	1.57×10^{12}	1.29×10^{12}
$^3P_1 \rightarrow {}^3P_0$	2.74×10^{11}	1.72×10^{11}	3.17×10^{11}	3.09×10^{11}	3.09×10^{11}	2.70×10^{11}	2.69×10^{11}	2.40×10^{11}	2.34×10^{11}	3.11×10^{11}
$^3P_0 \rightarrow {}^1D_2$	1.40×10^{6}	1.53×10^{6}	1.62×10^{6}	1.53×10^{6}	1.47×10^{6}	1.44×10^{6}	1.51×10^{6}	1.56×10^{6}	1.43×10^{6}	1.55×10^{6}
$^1D_2 \rightarrow {}^1G_4$	1.02×10^{1}	1.45×10^{1}	1.01×10^{1}	4.63	4.73	3.49	9.13	1.16×10^{1}	1.02×10^{1}	7.70
$^1G_4 \rightarrow {}^3F_4$	4.80×10^{6}	4.03×10^{6}	5.26×10^{6}	1.03×10^{7}	9.15×10^{6}	1.61×10^{7}	6.35×10^{6}	4.71×10^{6}	5.48×10^{6}	5.71×10^{6}
$^3F_4 \rightarrow {}^3F_3$	1.86×10^{12}	2.24×10^{12}	1.79×10^{12}	1.75×10^{12}	1.95×10^{12}	1.67×10^{12}	1.65×10^{12}	1.90×10^{12}	1.68×10^{12}	1.81×10^{12}
$^3F_3 \rightarrow {}^3F_2$	2.09×10^{10}	2.08×10^{10}	2.25×10^{10}	2.39×10^{10}	2.39×10^{10}	2.60×10^{10}	2.22×10^{10}	2.43×10^{10}	2.31×10^{10}	2.44×10^{10}
$^3F_2 \rightarrow {}^3H_4$	7.60×10^{3}	7.63×10^{3}	7.05×10^{3}	6.63×10^{3}	6.63×10^{3}	6.10×10^{3}	7.13×10^{3}	6.53×10^{3}	6.86×10^{3}	6.51×10^{3}

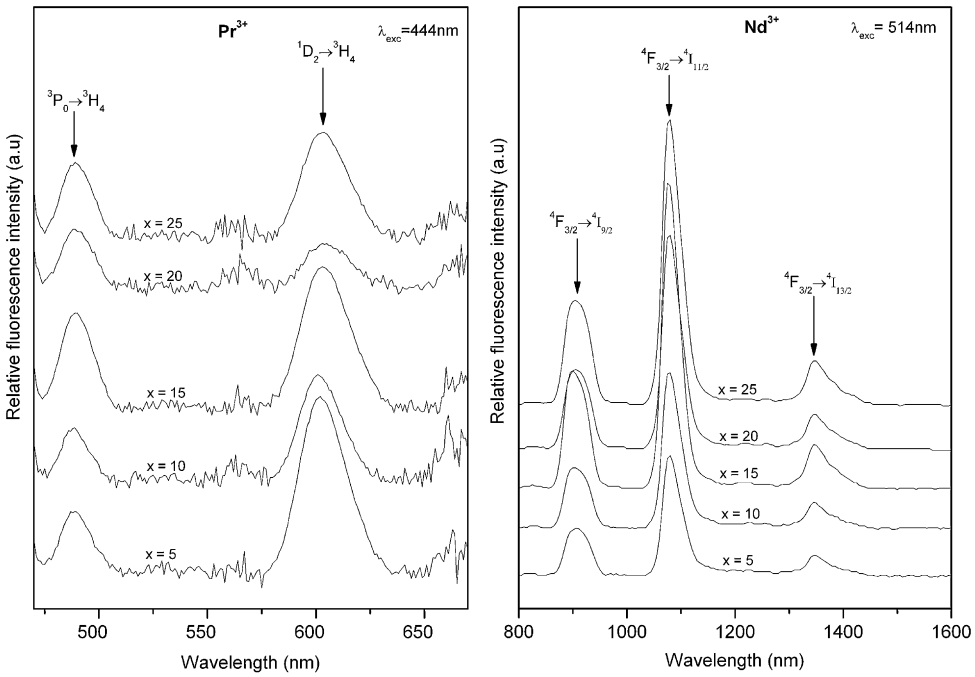

Fig. 6. Emission spectra of Pr^{3+} and Nd^{3+} doped lithium–sodium mixed alkali chloroborate glasses.

Table 7
Emission cross-sections (σ_P) of the observed emission transitions of Pr^{3+} and Nd^{3+} doped mixed alkali chloroborate glasses.

S. no.	Transition	Lithium–sodium					Lithium–potassium				
		$x=5$	$x=10$	$x=15$	$x=20$	$x=25$	$x=5$	$x=10$	$x=15$	$x=20$	$x=25$
Praseodymium											
1	$^3P_0 \rightarrow {}^3H_4$	0.225	0.047	1.301	1.785	1.413	1.809	1.217	1.174	1.066	0.531
2	$^1D_2 \rightarrow {}^3H_4$	0.445	0.919	0.547	0.857	1.718	1.056	0.879	0.818	0.553	0.801
Neodymium											
1	$^4F_{3/2} \rightarrow {}^4I_{9/2}$	0.96	1.33	1.40	1.50	1.56	1.19	0.92	1.35	1.22	1.46
2	$^4F_{3/2} \rightarrow {}^4I_{11/2}$	3.60	5.57	5.47	4.48	4.76	4.60	3.26	5.83	3.97	4.53
3	$^4F_{3/2} \rightarrow {}^4I_{13/2}$	1.16	2.15	1.91	1.56	1.62	1.77	1.02	2.33	1.76	1.31

imentally. Experimental and calculated branching ratios for the observed transitions are given in Table 8. It is observed that there is a good correlation between experimental and calculated branching ratios of the emission transitions of Nd^{3+} in the two glass matrices. But in the case of Pr^{3+} ion, some differences between experimental and calculated branching ratios are observed. Variation of emission intensities with x value in the glass matrices is shown in Fig. 7 for both Pr^{3+} and Nd^{3+} ions.

Table 8
Experimental (β_{exp}) and calculated branching ratios (β_{cal}) for observed emission transitions of Pr^{3+} and Nd^{3+} in lithium–sodium and lithium–potassium mixed alkali chloroborate glasses.

S. no	Transition	Parameter	Lithium–sodium					Lithium–potassium				
			$x=5$	$x=10$	$x=15$	$x=20$	$x=25$	$x=5$	$x=10$	$x=15$	$x=20$	$x=25$
Praseodymium												
1	$^3P_0 \rightarrow {}^3H_4$	β_{exp}	0.162	0.235	0.277	0.414	0.304	0.437	0.399	0.410	0.249	0.189
		β_{cal}	0.176	0.200	0.521	0.470	0.286	0.395	0.339	0.442	0.370	0.219
2	$^1D_2 \rightarrow {}^3H_4$	β_{exp}	0.837	0.765	0.722	0.586	0.695	0.562	0.660	0.589	0.751	0.810
		β_{cal}	0.304	0.297	0.370	0.344	0.345	0.300	0.308	0.388	0.260	0.309
Neodymium												
1	$^4F_{3/2} \rightarrow {}^4I_{9/2}$	β_{exp}	0.281	0.281	0.286	0.250	0.264	0.273	0.285	0.276	0.269	0.257
		β_{cal}	0.353	0.327	0.352	0.379	0.400	0.352	0.379	0.330	0.371	0.409
2	$^4F_{3/2} \rightarrow {}^4I_{11/2}$	β_{exp}	0.583	0.600	0.599	0.626	0.617	0.599	0.590	0.616	0.627	0.607
		β_{cal}	0.533	0.553	0.534	0.516	0.500	0.535	0.515	0.550	0.521	0.495
3	$^4F_{3/2} \rightarrow {}^4I_{13/2}$	β_{exp}	0.135	0.119	0.115	0.122	0.119	0.126	0.124	0.107	0.104	0.135
		β_{cal}	0.109	0.115	0.109	0.101	0.095	0.108	0.101	0.114	0.103	0.093

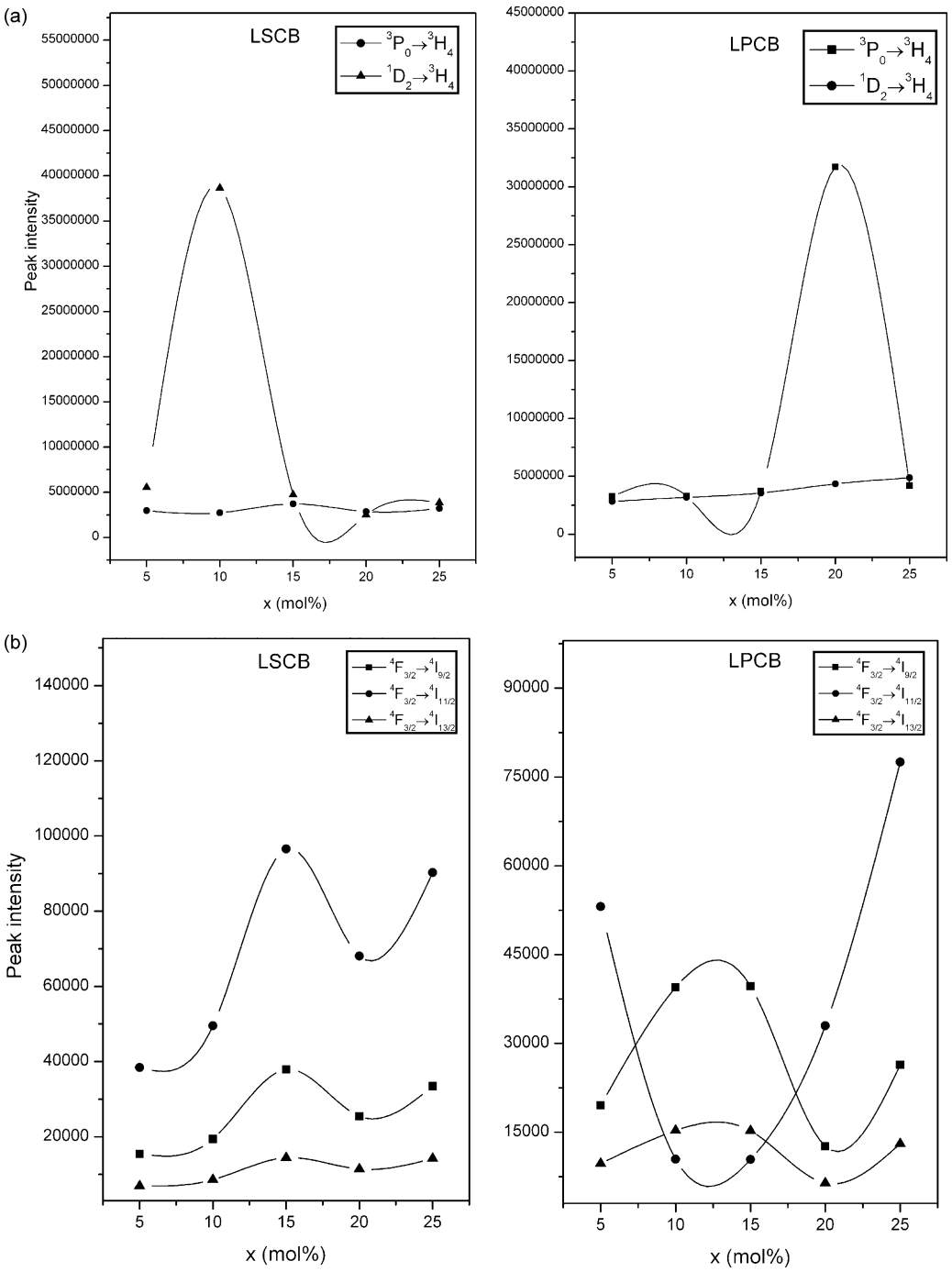

Fig. 7. (a) Variation of emission intensity with x in Pr^{3+} doped lithium–sodium (LSCB) and lithium–potassium (LPCB) mixed alkali chloroborate glasses. (b) Variation of emission intensity with x in Nd^{3+} doped lithium–sodium (LSCB) and lithium–potassium (LPCB) mixed alkali chloroborate glasses.

3.6. Optical band gaps

Optical band gaps (E_{opt}) for both direct and indirect transitions can be obtained following Davis and Mott theory [28] using the equation

$$\alpha(\omega) = B\frac{(\hbar\omega - E_{opt})^n}{\hbar\omega} \quad (2)$$

where $\alpha(w)$ is the absorption coefficient, B is a constant and E_{opt} is the optical band gap. For direct transitions $n = 1/2$ and for indirect transitions $n = 2$. From the plots of $(\alpha\hbar\omega)^2$ and $(\alpha\hbar\omega)^{1/2}$ as a function of photon energy $\hbar\omega$, E_{opt} values can be obtained for direct and indirect transitions respectively. The respective values of E_{opt} are obtained by extrapolating to $(\alpha\hbar\omega)^2 = 0$ for direct transitions and $(\alpha\hbar\omega)^{1/2} = 0$ for indirect transitions. The optical band gaps (in eV) of Pr^{3+} and Nd^{3+} doped two mixed alkali chloroborate glasses are given below.

x (in mol%)	Direct (Pr^{3+})		Indirect (Pr^{3+})		Direct (Nd^{3+})		Indirect (Nd^{3+})	
	LSCB	LPCB	LSCB	LPCB	LSCB	LPCB	LSCB	LPCB
5	3.12	3.15	3.00	3.05	3.21	3.32	3.09	3.18
10	2.88	3.14	2.87	3.05	3.16	2.53	2.97	2.48
15	3.23	3.06	2.92	2.98	2.91	3.09	2.76	3.07
20	3.12	3.13	3.04	3.06	3.19	3.23	2.97	3.03
25	3.10	3.10	2.98	3.00	3.33	3.04	3.04	2.90

From the above data it is observed that at $x = 15$ mol% (equal mol% of sodium and potassium) optical band gaps are increased in Pr^{3+} doped LSCB glass and decreased in LPCB glass. In the case of Nd^{3+} ion, at $x = 15$ mol%, optical band gaps are decreased in LSCB glass and increased in LPCB glass.

4. Conclusions

This research work presents the results of investigations on absorption and emission properties of Pr^{3+} and Nd^{3+} doped lithium–sodium and lithium–potassium mixed alkali chloroborate glasses. The Pr^{3+} ions show lower covalency at $x = 15$ mol% in lithium–sodium and lithium–potassium chloroborate glasses. The Nd^{3+} ions show lower covalency at $x = 20$ mol% in lithium–sodium and at $x = 10$ mol% in lithium–potassium mixed alkali glass matrices. Some structural changes have been observed at $x = 15$–20 mol% in Pr^{3+} doped lithium–sodium chloroborate glass and at $x = 5$–10 mol% in lithium–potassium chloroborate glass. In the case of Nd^{3+} ion, small structural changes are observed at $x = 10$–15 mol% in lithium–potassium chloroborate glass. The excited state, $^3F_3$ of Pr^{3+} ions show significantly higher radiative lifetimes in both the glass hosts. All the excited states of Nd^{3+} ions show higher radiative lifetimes at $x = 5$ mol% in lithium–sodium and at $x = 10$ mol% in lithium–potassium glass matrices. Among the two emission transitions of Pr^{3+} ion, the transition, $^3P_0 \rightarrow {}^3H_4$ has higher branching ratio at $x = 15$ mol% in lithium–sodium chloroborate glass. Among the three emission transitions of Nd^{3+} ion, the transition, $^4F_{3/2} \rightarrow {}^4I_{11/2}$ has higher branching ratio at $x = 10$ mol% in lithium–sodium chloroborate glass and at $x = 15$ mol% in lithium–potassium chloroborate glass. The emission cross-section for the transition, $^3P_0 \rightarrow {}^3H_4$ of Pr^{3+} ions is higher at $x = 5$ mol% in lithium–potassium chloroborate glass. In the case of Nd^{3+} ions, the transition, $^4F_{3/2} \rightarrow {}^4I_{11/2}$ has higher emission cross-section at $x = 15$ mol% in lithium–potassium chloroborate glass and these transitions are favorable for laser excitation.

Acknowledgements

Y.C.R. expresses his thanks to the University Grants Commission for providing financial assistance in the form of major research project.

References

[1] M. Dejneka, B. Samson, Mater. Res. Soc. Bull. 24 (1999) 39.
[2] M.J. Weber, J. Non-Cryst. Solids 42 (1980) 189.
[3] A. Florez, O.L. Malta, Y. Messaddeq, M.A. Aegerter, J. Non-Cryst. Solids 213–214 (1997) 315.
[4] S. Nicolas, E. Descroix, M.F. Joubert, Y. Guyot, M. Laroche, R. Moncorge, R.Yu. Abdulsabirov, A.K. Naumov, V.V. Sesmashko, A.M. Tkachuk, M. Malinowski, Opt. Mater. 22 (2003) 139.
[5] Yu. Zorenko, V. Gorbenko, I. Konstankevych, A. Voloshinovskii, G. Stryganyuk, V. Mikhailin, V. Kolobanov, D. Spassky, J. Lumin. 114 (2005) 85.
[6] B.J. Pask, H.S. Seo, J.T. Ahn, Y.G. Choi, D.Y. Jeon, W.J. Chung, J. Lumin. 128 (2008) 1617.
[7] W. Koechner, Solid State Laser Engineering, Springer-Verlag, Berlin, 1996.
[8] R. Scheps, Appl. Opt. 28 (1989) 89.
[9] N.P. Barnes, M.E. Storm, P.L. Cross, M.W. Skolout Jr., J. Quantum Electron 26 (1990) 558.
[10] D.E. Day, J. Non-Cryst. Solids 21 (1976) 343.
[11] A.H. Dietzel, Phys. Chem. Glasses 24 (1983) 172.
[12] M. Ingram, Glastech. Ber. Sci. Technol. 67 (1994) 151.
[13] B. Roling, M.D. Ingram, J. Non-Cryst. Solids 265 (2000) 113.
[14] G. Domimak-Dzik, W. Ryba-Romanowski, J. Pisarska, W.A. Pisarski, J. Lumin. 122 (2007) 62.
[15] P. Maass, A. Bunde, M.D. Ingram, Phys. Rev. Lett. 68 (1992) 3064.
[16] J.E. Shelby, J. Am. Ceram. Soc. 66 (1983) 414.
[17] B.R. Judd, Phys. Rev. 127 (1962) 750.
[18] G.S. Ofelt, J. Chem. Phys. 37 (1962) 511.
[19] Y.C. Ratnakaram, A. Vijaya Kumar, R.P.S. Chakradhar, J. Lumin. 118 (2006) 227.
[20] Y.C. Ratnakaram, D. Thirupathi Naidu, A. Vijaya Kumar, J.L. Rao, J. Phys: Condens. Matter 16 (2004) 3779.
[21] M.B. Saisudha, J. Ramakrishna, Phys. Rev. B 53 (10) (1996) 6186.
[22] E.W.J.L. Oomen, A.M.A. van Dongen, J. Non-Cryst. Solids 111 (1989) 205.
[23] H. Takebe, K. Monnaya, T. Izumitani, J. Non-Cryst. Solids 178 (1994) 58.
[24] M. Shojiya, Y. Kawamoto, K. Kadono, J. Appl. Phys. 89 (2001) 4944.
[25] M. Shojiya, M. Takahashi, R. Kanno, Y. Kawamoto, K. Kadono, J. Appl. Phys. 82 (1997) 6259.
[26] M. Yamane, Y. Asahara, Glasses for Photonics, Cambridge University, Cambridge, 2000.
[27] L. Srinivasa Rao, M. Srinivasa Reddy, M.V. Ramana Reddy, N. Veeraiah, Physica B 403 (2008) 2542.
[28] F.A. Davis, N.F. Mott, Philos. Mag. 22 (1970) 903.